

Spectral Minutiae for Vein Pattern Recognition

Daniel Hartung

Norwegian Information Security Laboratory (NISlab)
Høgskolen i Gjøvik, Teknologivn. 22, 2815 Gjøvik, Norway

daniel.hartung@hig.no

Martin Aastrup Olsen

Center for Advanced Security Research Darmstadt (CASED)
Mornewegstrasse 32, 64293, Darmstadt, Germany

martin.olsen@cased.de

Haiyun Xu

University of Twente
PO Box 217, 7500 AE Enschede, The Netherlands

h.xu@ewi.utwente.nl

Christoph Busch

Norwegian Information Security Laboratory (NISlab)
Høgskolen i Gjøvik, Teknologivn. 22, 2815 Gjøvik, Norway

christoph.busch@hig.no

Abstract

Similar to biometric fingerprint recognition, characteristic minutiae points – here end- and branch points – can be extracted from skeletonized veins to distinguish individuals. An approach to extract those vein minutiae and to transform them into a fixed-length, translation and scale invariant representation where rotations can be easily compensated is presented in this paper. The proposed solution based on spectral minutiae is evaluated against other comparison strategies on three different datasets of wrist and palm vein samples. It shows a competitive biometric performance while producing features that are compatible with state-of-the-art template protection systems.

1. Introduction

Thought to be a robust approach for liveness detection in fingerprint and hand geometry systems, vein recognition evolved to an independent biometric modality over the last decade [3]. Vein recognition systems are exploiting specific light absorption properties of deoxygenated blood flowing in subcutaneous blood vessels. Because venous blood absorbs the near infrared light emitted by LEDs in the vein

sensor, the veins become visible as dark tubular structures on the image. Alternatively a far infrared approach – where heat radiation of the blood vessels is measured – can be used [19]. Vein patterns evolve during the embryonic vasculogenesis. Their final structure is mostly influenced by random factors [8]. Even though scientific research about the uniqueness of vein patterns is sparse, many resources state that vein patterns are unique among individuals [2, 21]. It is also expected, that the position of veins is constant over a whole lifetime [6]. Offering the same user convenience as fingerprints while being highly secure against spoofing, vein recognition has been applied in different fields of access control during the last years. Because vein scanners work contact-less they are considered to be more hygienic than systems requiring direct physical contact. This makes vein recognition particularly suited for applications in public environments.

Due to the fact, that the network of blood vessels forming the vein patterns is located underneath the skin, a person's individual vein patterns is hard to forge; no latent prints are left unintentionally. Besides this privacy protecting property, there are also privacy concerns reported in vein recognition systems since disease patterns can be read from the biometrics information [10]. There are some attempts to prevent the proliferation of sensitive data from biometric

references, to overcome the linkability between different databases and to enable revocation capacities so that multiple identifiers can be constructed from the same biometric trait. It is not sufficient to simply encrypt biometric templates with classic cryptographic functions since they can not be compared in the encrypted domain. The goal is to introduce pseudonymous identifiers that cannot be tracked back to the data subject and multiple pseudonymous identifiers of the same data subject cannot be linked against each other.

A recent overview of existing biometric template protection systems is given in [4]. The described harmonized reference architecture is integrated in the international standard ISO/IEC 24745 *Biometric Information Protection* and its nomenclature is used throughout this paper. The Fuzzy Commitment Scheme [11] is one of the systems for template protection, it introduced shielding functions to secure biometric data. The Helper Data Scheme (HDS) [17] that uses the principle of fuzzy commitments to privacy protect biometric features and satisfy the above-mentioned requirements is an extension of classic biometric systems where the extracted feature vectors are further processed. One requirement on the feature vectors is that they are of fixed length and structure, so that components can be analyzed for reliability and can consistently be reconstructed from biometric data.

This paper is describing a feature extraction method for vein patterns based on minutiae points, known from fingerprint recognition, where the position of end- and branch points from the skeletal representation of vein patterns are being used. These feature points can – due to noise from various sources like the sensor, the biometric trait, or the preprocessing – not be reconstructed perfectly; their amount and their position will vary. To overcome these issues and to make the features compatible with the HDS for template protection, an approach called *spectral minutiae* is applied to the original vein minutiae. This approach was applied very successfully to fingerprint minutiae [20].

In [12] a hand vein based authentication system using Delaunay triangulation of these minutiae is presented. The approach is based on the extraction of minutia groups to form triplets as well as a triplet type determined from the composition of endpoints and bifurcations. The resulting rotation and translation invariant feature vector is variable in length as determined by the number of identified triplets. As a fixed-length feature vector is a prerequisite for HDS the Delaunay triangulation method is not suitable in this context.

The structure of the paper is as follows: beginning with the introduction of the vein pattern preprocessing and feature extraction system in section 2, the approach of mapping those features into a fixed-length, translation and scale invariant representation is given in section 3. The follow-

ing section 4 is showing the feasibility of the approach with experiments, there details about the database and the performance evaluation can be found. The last section concludes the paper and points out future work.

2. Proposed Biometric Vascular Pattern Recognition System

The biometric system based on vein data is going to be introduced in this section. One challenge in vein recognition systems is to cope with noisy and low contrast images caused by the sensor. Vein image quality is subject to several factors like ambient light, air temperature, skin color and varying thicknesses of the fingers. As a result of all these factors the sensor delivers images suffering from an unfavorable signal to noise ratio, low contrast and non-uniform brightness. The vein recognition system has to cope with global and local contrast changes in the image, while suppressing noise. Therefore sophisticated image processing is indispensable in order to improve the images. The enhanced images must be segmented before an image skeleton representing the topological structure of the data subject's veins can be extracted. Minutiae feature points are extracted from the skeleton and will form the input to the spectral minutiae post processing which is introduced in section 3.

2.1. Preprocessing

The proposed solution is not performing a region of interest (ROI) selection to be as generic as possible. Therefore the first step in the preprocessing pipeline is the contrast enhancement. For the proposed system the images are first enhanced by using adaptive non-local means, successfully applied to face recognition in [15], followed by the noise suppressing and edge enhancing nonlinear diffusion algorithm [1]. At this point the image is inverted such that veins now appear as high intensity pixels, while tissue between the veins appear as low intensity. The results of the algorithm applied to a raw wrist vein image can be seen in Figure 1(b).

2.2. Segmentation

The multi-scale filter method by Frangi et. al. [9], designed for simultaneous noise and background suppression in medical imaging of vessels, is used as a segmentation method on the vein images. The method searches for tubular structures in the image by analyzing the second order information (Hessian). The second order derivative of a Gaussian kernel generates a probe kernel that can measure contrast inside a defined range in the direction of the derivative. An eigenvalue analysis of the Hessian gives the direction of smallest curvature and therefore the direction of the vessel, the eigenvalues can be used to classify pixels as vessel

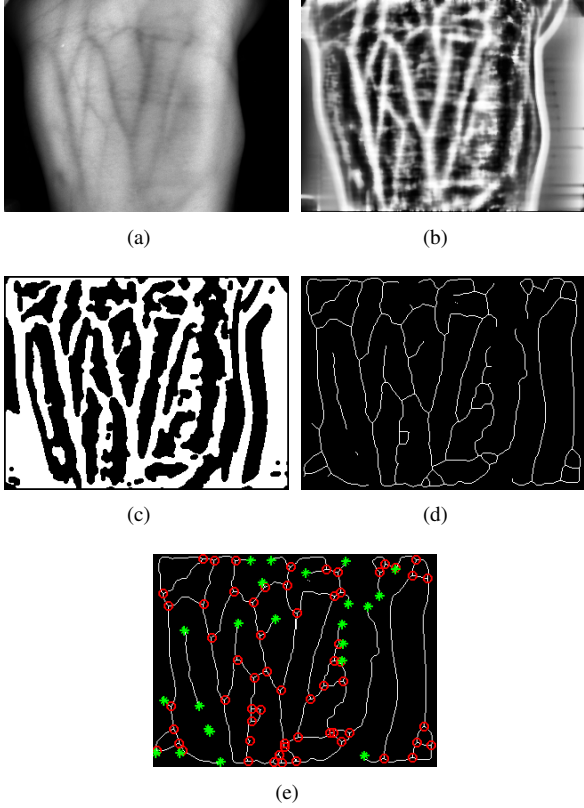


Figure 1. Sample wrist vein image [14] after different stages of the preprocessing pipeline of the proposed system: (a) raw, cropped vein image; (b) contrast enhanced image; (c) segmentation of an optimized vein pattern image; (d) skeletonization of segmented image; (e) overlay of extracted minutiae points and skeleton. Green stars: endpoints, red circles: branch points

or background. Figure 1(c) shows the effect of the method applied to the optimized image.

2.3. Skeletonization

Skeletons are extracted by the fast marching skeletonization algorithm [16]. One advantage is the built-in pruning method, which allows cutting off certain branches from the image skeleton. In fast marching skeletonization incremental indices are assigned to each pixel on the edge of the figure. Then they are collapsed until only the center line remains. From the difference between two neighboring indices, it can be concluded, how close a skeleton branch is to the center of the figure. The difference between indices at fine-grained branches at the edge of the image skeleton is small, whereas it is large in the center part. These fine-grained branches are most likely artifacts, which were introduced by segmentation errors or noise and can be removed by applying a threshold. All skeleton points where the difference between their indices falls below the threshold are deleted. All other points are kept. Hence, depending on the

threshold, more or less of these remote branches are cut off. One example is shown in figure 1(d).

2.4. Feature Point Detection

After extracting the skeletal representation from a vein image, the specific feature points have to be extracted. An efficient and reliable method based on a convolution approach is proposed in [13] and is used here. It is based on convoluting the binary image with a filter consisting of unique power of two values to get unique filter responses for every pattern in the mask size. The end- as well as the branch points of the vascular skeleton can be found by searching for their pre-computed filter response values in the filter response of the image. The extracted minutiae points are overlayed with the corresponding skeleton in Figure 1(e).

3. Spectral Minutiae

The *spectral minutiae* representation is a method to represent a fingerprint minutiae set as a fixed-length feature vector, which is invariant to translation, rotation and scaling. These characteristics enable the combination of fingerprint recognition systems with template protection schemes based on the HDS and allow for fast minutiae-based matching as well. Considering the similar characteristics of the vein minutiae and fingerprint minutiae patterns, we applied this method to the vein minutiae features, in order to be able to combine vein pattern recognition with the HDS based template protection schemes.

In this paper, we applied the *location-based spectral minutiae representation* (SML) approach presented in [20] in order to code the vein minutiae location information. We first give an overview of the SML approach.

3.1. SML Approach

Assume we have a fingerprint or vein pattern with Z minutiae. In SML, we code the minutiae locations by indicator functions,

$$m(x, y; \sigma_L^2) = \sum_{i=1}^Z \frac{1}{2\pi\sigma_L^2} \exp\left(-\frac{(x - x_i)^2 + (y - y_i)^2}{2\sigma_L^2}\right), \quad (1)$$

with (x_i, y_i) the location of the i -th minutia in the image. Thus, in the spatial domain, each minutia is represented by an isotropic two-dimensional Gaussian function, illustrated in figure 2(b).

Taking the Fourier transform of $m(x, y; \sigma_L^2)$ and keeping only the magnitude of the Fourier spectrum (in order to make the spectrum invariant to translation of the input), we obtain the location-based spectral minutiae representation

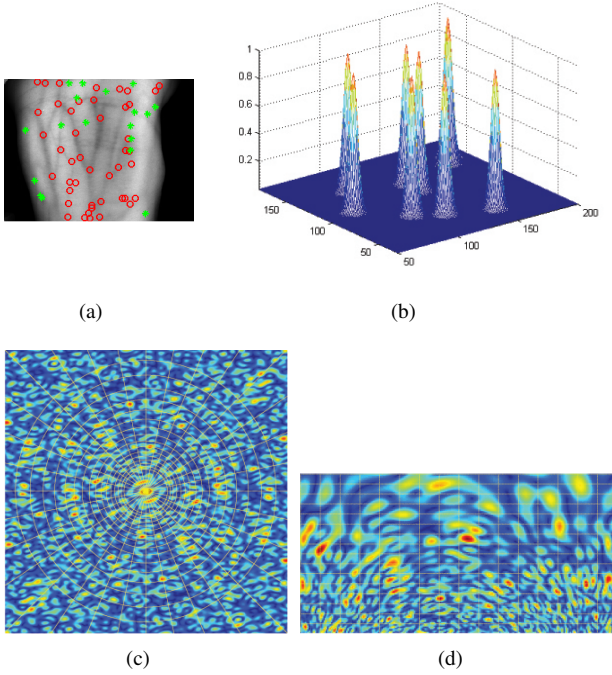


Figure 2. Illustration of the SML representation procedure. (a) vein pattern and its minutiae points; (b) representing minutiae points as isotropic two-dimensional Gaussian functions. (c) the Fourier spectrum in a Cartesian coordinate and a polar-logarithmic sampling grid. (d) the Fourier spectrum sampled on a polar-logarithmic grid.

$$\mathcal{M}_L(\omega_x, \omega_y; \sigma_L^2) = \left| \exp\left(-\frac{\omega_x^2 + \omega_y^2}{2\sigma_L^2}\right) \sum_{i=1}^Z \exp(-j(\omega_x x_i + \omega_y y_i)) \right|. \quad (2)$$

In order to obtain the final spectral representations, the continuous spectra SML (2) need to be sampled on a polar-logarithmic grid. A polar mapping transforms rotation to translation in the horizontal direction, while a logarithmic mapping transforms scaling to translation in the vertical direction. In the radial direction λ , we use $M = 128$ samples between λ_l and λ_h . In the angular direction β , we use $N = 256$ samples uniformly distributed between $\beta = 0$ and $\beta = \pi$. A polar-logarithmic sampling process is illustrated in Figures 2(c) and 2(d).

3.2. Comparison

Two different comparison strategies are considered, the direct matching and the fast rotation shift search. They are described in this section.

3.2.1 Direct Matching

Let $R(m, n)$ and $T(m, n)$ be the two sampled minutiae spectra in the polar-logarithmic domain respectively achieved from the *reference* sample and *test* sample – originating from a fingerprint or a vein source. Both $R(m, n)$ and $T(m, n)$ are normalized to have zero mean and unit energy. As a similarity score, the normalized cross-correlation with zero lag of two minutiae spectra was chosen, which is a common similarity measure in image processing. Therefore, the SML correlation (SMLC) as similarity score between R and T is defined as:

$$S_{DM}^{(R,T)} = \frac{1}{MN} \sum_{m,n} R(m, n)T(m, n). \quad (3)$$

3.2.2 Fast Rotation Shift Searching

Rotations might not only be a problem in fingerprint recognition but as well in vein recognition, depending on the capture device used for the acquisition. The fast rotation shift search algorithm makes a costly normalization of the minutiae points unnecessary by compensating for rotations by testing several rotated spectra. Because we applied the polar-logarithmic transform to the Fourier spectra, the rotation becomes the circular shift in the horizontal direction in our minutiae spectra. We chose to test rotations from -10° to $+10^\circ$ as starting points, which corresponds to circular shifts from -15 units to +15 units in the polar-logarithmic domain.

Let $T_k(m, n)$ be defined as $T(m, n)$ with a circular shift k in the horizontal direction. For each shift trial, a new similarity score $S^{(R,T_k)}$ is calculated using (3). Finally, the highest score is chosen as the similarity score and the corresponding shift k is recorded as the best shift (that is, the best rotation).

We applied a fast search for the best shift. This algorithm consists of the following steps:

- (1) 5 circular shifts ($k = -12, -6, 0, 6, 12$) are applied to $T(m, n)$ and the similarity scores $S^{(R,T_k)}$ are calculated. The maximum value of $S^{(R,T_k)}$ is denoted as S_1 and its corresponding shift k is denoted as k_1 ;
- (2) 2 circular shifts ($k = k_1 - 2, k_1 + 2$) are applied to $T(m, n)$, and the similarity scores $S^{(R,T_k)}$ are calculated. The maximum value of $S^{(R,T_k)}$ and S_1 is denoted as S_2 , and its corresponding shift k is denoted as k_2 ;
- (3) 2 circular shifts ($k = k_2 - 1, k_2 + 1$) are applied to $T(m, n)$, and the similarity scores $S^{(R,T_k)}$ are calculated. The maximum value of $S^{(R,T_k)}$ and S_2 is denoted as S_{final} .

Using this fast rotation shift search algorithm, only 9 shift trials need to be tested, instead of 31 shift trials for an exhaustive search. After these steps, the value S_{final} is recorded as the final similarity score between R and T .

4. Experiments

The simulations are designed to examine the performance – measured in Equal Error Rates – of different comparison strategies used in vein recognition. Three datasets, which main properties are described in Table 1, will give a broad basis for conclusions about the proposed approach of using spectral minutiae as features.

4.1. Databases

The *SNIR* and *SFIR* databases were gathered in 2006 in Singapore's Nanyang Technological University and contain a subset of samples that were used in several publications [18, 19]. The two parts contain 732 back hand vein samples in the near infrared and 173 in the far infrared spectrum from 122 respectively 34 data subjects.

A third database *UC3M* is used for the experiment, it was collected in 2010 in the University Carlos III of Madrid. The dataset consists of 348 vein images in the near infrared spectrum from the wrist area of 29 data subjects.

One limitation of the datasets is that they are captured during only one session, which limits the variability in the signals.

4.2. Comparison Strategies

Table 2 shows the comparison strategies used in the simulations, those are: Hausdorff distance, Modified Hausdorff (MHD) [19, 7], Similarity-based Mix-matching (SMM)[5] and the proposed SML correlation (SMLC) as well as the SML fast rotate (SMLFR) strategy.

The selection of comparison strategies covers a range of different features that are used, the Hausdorff as well as the MHD algorithms use the location of the minutiae points directly. The SML algorithm introduced in Section 3 works with the spectral minutiae representation of the minutiae location. The approaches are introduced in detail in Section 3.2.

The SMM algorithm proposed by Chen et al. uses geometrical properties of image skeletons and segmented images to overcome problems with affine transformations. Similarity-based Mix-matching, compensates small translation and rotation errors by comparing the segmented version of the reference sample with the image skeleton of the test sample. The computational effort is higher than the feature point based approaches.

For the simulations all minutiae point locations are used as one concatenated feature vector, not distinguishing between end- or branch points.

4.3. Performance Evaluation

The evaluation is based on database simulations using the Equal Error Rate (EER) as metric, the proposed system of preprocessing and feature point detection from Section 2 is used. During the skeletonization approach using

the fast marching algorithm the images from the UC3M database are pruned using a radial threshold of 15, whereas the threshold was set to 75 for the other datasets, which showed good results on the stability of the skeletons.

Within the simulations the maximum number of genuine comparisons as indicated in Table 1 and all imposter comparisons were taken into account for the EER calculations and plots.

All the simulation results are summarized in Table 2. The Receiver Operation Characteristics (ROC) are plotted in Figure 3, Hausdorff performance is not included for obvious reasons.

Comparison	SNIR	SFIR	UC3M
Hausdorff	34.65%	25.84%	42.50%
MHD [†]	1.13%	3.88%	10.61%
SMM [‡]	0.14%	1.24%	1.18%
SMLC	1.35%	3.60%	6.13%
SMLFR	1.62%	4.33%	5.90%

Table 2. Evaluation of the proposed solution in comparison to other comparison strategies in Equal Error Rates. [†]Modified Hausdorff distance as proposed in [19, 7]. [‡]Similarity-based Mix-matching [5].

In addition to the performance evaluation statistical information regarding the number of extracted minutiae, as well as the skeletons were extracted and summarized in Table 3.

Property	SNIR	SFIR	UC3M
Avg. # of Endpoints	16.42	18.32	62.01
Avg. # of Branch points	56.93	28.82	87.21
Avg. Skeleton length	3146.23	2157.4	3594.62

Table 3. Statistics about the average number of end and branch points, as well as the average skeleton length (in pixels) for the different datasets.

5. Conclusions

From the simulations we can see, that the proposed system for vein pattern recognition is able to extract features of reasonable quality for all datasets. The evaluation states a performance of the spectral minutiae approach at the same level as reference measures based on point-to-point comparisons like the MHD, and in the case of the UC3M dataset both SMLC and SMLFR exceed MHD performance; the simple Hausdorff distance measure does not give satisfactory results on any of the data sets. Only the computationally more complex SMM approach, that works on the skeleton and image level, can outperform the proposed solution.

Property	SNIR	SFIR	UC3M*
Frequency Band	NIR	FIR	NIR
Modality	Back of Hand (2)	Back of Hand (2)	Wrist (2)
Data Subjects	122	34	29
Sessions		1	
Images per Session	2×3	$2 \times \sim 3$	2×6
Images	732	173	348
Genuine Comparisons	732	169	870
Resolution (px)	$(644 \times 492)^\perp$	320×240	$(640 \times 480)^\perp$
Depth		8 Bit gray-scale	

Table 1. Properties of the biometric vein datasets used in the experimental section. *Details published in [14]. $^\perp$ Image size reduced by 50% in each dimension for experiments.

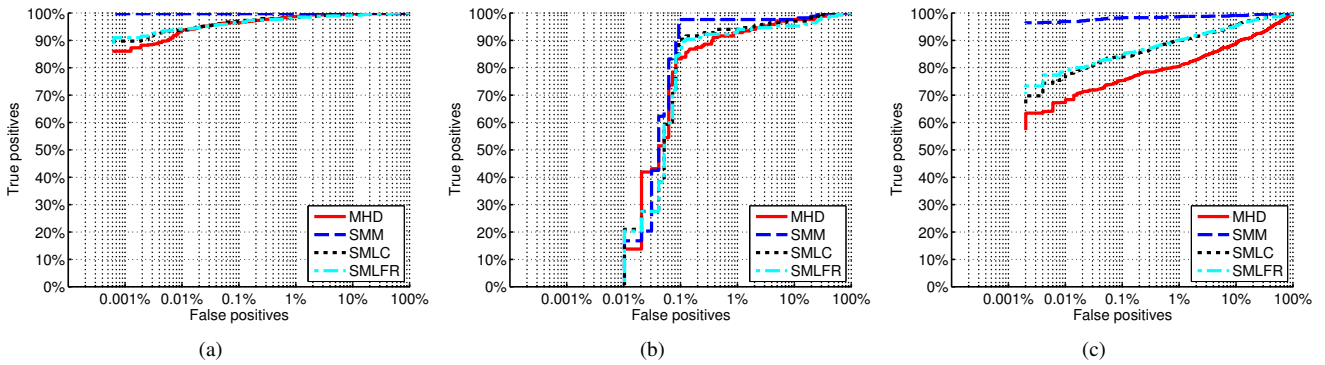


Figure 3. Receiver Operation Characteristics from the databases: (a) SNIR, (b) SFIR, (c) UC3M.

The fast rotation comparison is not improving the performance compared to the direct correlation measure, it can be assumed that the samples are only fairly rotated to each other. This can be due the fact that the databases are gathered during only one session without drastic changes of the hand position or due to the sensor layout.

It can be stated, that the proposed solution stays competitive in performance compared to other point-to-point based approaches with the additional advantage of producing fixed-length feature vectors, that are compatible with state-of-the-art template protection systems. Future work is focused on combining the biometric modality of vein recognition, where the sensitive information is hidden inside the body, with the proposed system and the Helper Data Scheme – as a privacy enhancing technology – resulting in a secure system fulfilling strict legislative requirements and user expectations regarding privacy.

Acknowledgments

The authors would like to thank our supervisors for guidance and support, and Nanyang Technological University and University Carlos III of Madrid for making their vein pattern data sets available to the research community.

References

- [1] *Applications of Nonlinear Diffusion in Image Processing and Computer Vision*, volume Vol. LXX. Acta Math. Univ. Comenianae, 2001. 2
- [2] A. M. Badawi. Hand vein biometric verification prototype: A testing performance and patterns similarity. In *IPCV*, pages 3–9, 2006. 1
- [3] R. Bolle and S. Pankanti. *Biometrics, Personal Identification in Networked Society: Personal Identification in Networked Society*. Kluwer Academic Publishers, Norwell, MA, USA, 1998. 1
- [4] J. Breebaart, C. Busch, J. Grave, and E. Kindt. A reference architecture for biometric template protection based on pseudo identities. In *BIOSIG*, pages 25–38, 2008. 2
- [5] H. Chen, G. Lu, and R. Wang. A New Palm Vein Method Based on ICP Algorithm. In *International Conference on Informaion Systems*, November 2009. 5
- [6] R. Derakhshani, A. Ross, and S. Crialmeanu. A New Biometric Modality Using Conjunctival Vasculature. In *Proceedings of Artificial Neural Networks in Engineering*, November 2006. 1
- [7] M.-P. Dubuisson and A. Jain. A modified hausdorff distance for object matching. In *Pattern Recognition, 1994. Vol. 1 - Conference A: Computer Vision Image Processing., Proceedings of the 12th IAPR International Conference on*, volume 1, pages 566–568 vol.1, oct 1994. 5

- [8] A. Eichmann, L. Yuan, D. Moyon, F. Lenoble, L. Pardanaud, and C. Brant. Vascular Development: From Precursor Cells to Branched Arterial and Venous Networks. *International Journal of Developmental Biology*, 49:259–267, 2005. 1
- [9] R. F. Frangi, W. J. Niessen, K. L. Vincken, and M. A. Viergever. Multiscale Vessel Enhancement Filtering. In *Medical Image Computing and Computer-Assisted Intervention*, pages 130–137. Springer-Verlag, 1998. 2
- [10] D. Hartung and C. Busch. Why vein recognition needs privacy protection. *Intelligent Information Hiding and Multimedia Signal Processing, International Conference on*, 0:1090–1095, 2009. 1
- [11] A. Juels and M. Wattenberg. A fuzzy commitment scheme. In *ACM Conference on Computer and Communications Security*, pages 28–36, 1999. 2
- [12] A. Kumar and K. V. Prathyusha. Personal authentication using hand vein triangulation and knuckle shape. *Trans. Img. Proc.*, 18:2127–2136, September 2009. 2
- [13] M. A. Olsen, D. Hartung, C. Busch, and R. Larsen. Convolution approach for feature detection in topological skeletons obtained from vascular patterns. In *IEEE Symposium Series on Computational Intelligence 2011*, Apr 2011. 3
- [14] S. Pascual, J.E., Uriarte-Antonio, J., Sanchez-Reillo, R., and M. Lorenz. Capturing Hand or Wrist Vein Images for Biometric Authentication Using Low-Cost Devices. In *Intelligent Information Hiding and Multimedia Signal Processing (IIH-MSP), 2010 Sixth International Conference on*, pages 318 –322, october 2010. 3, 6
- [15] V. Struc and N. Pavesic. Illumination Invariant Face Recognition by Non-local Smoothing. In *Proceedings of the BIODID Multicomm*, September 2008. 2
- [16] A. Telea and J. J. van Wijk. An Augmented Fast Marching Method for Computing Skeletons and Centerlines. In *Joint Eurographics - IEEE TCVG Symposium on visualization*, 2002. 3
- [17] P. Tuyls and J. Goseling. Capacity and examples of template-protecting biometric authentication systems. In *Biometric Authentication*, volume 3087 of *Lecture Notes in Computer Science*, pages 158–170. Springer Berlin / Heidelberg, 2004. 2
- [18] L. Wang and G. Leedham. Computational intelligence and security. chapter A Watershed Algorithmic Approach for Gray-Scale Skeletonization in Thermal Vein Pattern Biometrics, pages 935–942. Springer-Verlag, Berlin, Heidelberg, 2007. 5
- [19] L. Wang, G. Leedham, and D. S.-Y. Cho. Minutiae feature analysis for infrared hand vein pattern biometrics. *Pattern Recognition*, 41(3):920 – 929, 2008. Part Special issue: Feature Generation and Machine Learning for Robust Multimodal Biometrics. 1, 5
- [20] H. Xu, R. N. J. Veldhuis, A. M. Bazen, T. A. M. Kevenaar, T. A. H. M. Akkermans, and B. Gokberk. Fingerprint verification using spectral minutiae representations. *Trans. Info. For. Sec.*, 4:397–409, September 2009. 2, 3
- [21] T. Yanagawa, S. Aoki, and T. Ohyama. Human finger vein images are diverse and its patterns are useful for personal identification. MHF Preprint Series, Faculty of Mathematics, Kyushu University, Fukuoka JAPAN, 2007. 1